



# STITCH Analysis, ADMET Profiling, Molecular Docking, DFT, and Molecular Dynamics of Compound from *Eleutherine americana* L. Merr as Cyclooxygenase-2 Inhibitor

Ayu Faadila, Wiji Utami\*, Aisyah

Chemistry Department, Faculty of Science and Technology, UIN Sulthan Thaha Saifuddin, Jambi, 36361, Indonesia

\* Corresponding author: [wijiutami@uinjambi.ac.id](mailto:wijiutami@uinjambi.ac.id)

<https://doi.org/10.14710/jksa.29.2.132-148>



## Article Info

### Article history:

Received: 19<sup>th</sup> November 2025

Revised: 16<sup>th</sup> February 2026

Accepted: 19<sup>th</sup> February 2026

Online: 14<sup>th</sup> March 2026

### Keywords:

Anti-inflammatory; Dayak Onion; COX-2; Molecular Docking; Molecular Dynamics

## Abstract

Dayak onion (*Eleutherine americana* (L.) Merr) is known to have potential as an inflammatory pathway modulator as it contains active compounds such as eleutherine, isoeleutherine, and eleutol. They are known to have anti-inflammatory, antioxidant, and anti-cancer activities. This study explored the potential of *Eleutherine americana* (L.) Merr bioactive compounds as COX-2 enzyme inhibitors using an in silico approach. The data were obtained using Lipinski's rule of 5, ADMET profile prediction, molecular docking, and molecular dynamics simulation. The molecular docking results showed that eleutherin, isoeleutherin, and elecanacin had strong binding affinities of -8.09, -8.19, and -8.06 kcal/mol to the active site of COX-2 with amino acid residues SER530, ALA527, SER353, HIS90, PHE518, LEU384, and PHE381. Meanwhile, MD analysis showed that eleutherin formed stable RMSD C $\alpha$  interactions at a distance of 1.4 Å for 100 ns with COX-2, while isoeleutherin showed slight fluctuations of 2.5 Å at 75 ns with an average radius of gyration of 24 Å. The findings demonstrate potential for further development, particularly in the exploration of new herbal-based drug discovery using *Eleutherine americana* (L.) Merr, and can be studied further in vitro and in vivo to validate the drug candidate as a COX-2 inhibitor in anti-inflammatory therapy.

## 1. Introduction

The World Health Organization reports in 2021 that inflammation is the greatest threat to human health, with 3 out of 5 people worldwide dying from chronic inflammation, such as stroke, heart disease, and respiratory disorders [1]. Inflammation refers to the body's physiological response to tissue damage or infection, characterized by the release of cytokines and prostaglandins [2]. Prostaglandin production is catalyzed by cyclooxygenase (COX), which consists of the isoforms COX-1 and COX-2. The COX-2 isoform is induced when the body is exposed to pathogens, and its increased expression can cause acute and chronic inflammation, including cancer, arthritis, and cardiovascular disorders. If inflammation is not properly treated, it can lead to progressive tissue damage and worsen the patient's condition. Therefore, inhibiting COX-2 enzyme activity is

a therapeutic strategy to control inflammation and prevent more serious disease complications [3].

Current treatment for inflammation still widely uses Non-Steroidal Anti-Inflammatory Drugs (NSAIDs) such as ibuprofen, aspirin, celecoxib, diclofenac, diflunisal, etodolac, fenoprofen, flurbiprofen, indomethacin, ketoprofen, ketorolac, mefenamic acid, meloxicam, nabumetone, naproxen, oxaprozin, piroxicam, sulindac, tolmetin, which are approved by the United States Food and Drug Administration (USFDA) [4]. However, long-term use of NSAIDs can cause side effects such as indigestion, pain, diarrhea, bleeding, gastrointestinal disorders, stomach ulcers, and an increased risk of cardiovascular disease. Thus, although effective in inhibiting COX-2, it poses a high safety risk. It indicates that there is still a need to develop alternative inhibitors from secondary metabolites of herbal plants with a broad

spectrum of bioactivity and comparable effectiveness, with a lower risk of side effects [5].

As modern research develops, traditional plants are increasingly being explored for their potential as sources of bioactive compounds. Various secondary metabolites from plants, such as flavonoids, alkaloids, terpenoids, and naphthoquinones, have been shown to have broad pharmacological activities, including anti-inflammatory properties. Therefore, exploration of traditional Indonesian plants has the potential to produce new anti-inflammatory drug candidates that are safer and more effective [6]. Dayak onion (*Eleutherine americana* (L.) Merr) is one of Kalimantan's distinctive medicinal plants widely used to treat various diseases, including infections, diabetes, cancer, and inflammation. Several studies have reported the biological activity of *Eleutherine americana* (L.) Merr acts as an antioxidant, antibacterial, and antitumor agent [7].

Hardi *et al.* [8] reported that *Eleutherine americana* extract suppresses inflammation by up to 72.74% in red blood cell membrane stability. In vitro, the ethyl acetate fraction of *Eleutherine americana* (L.) Merr tubers had the highest antioxidant activity at an  $IC_{50}$  value of  $26.98 \pm 0.507$   $\mu\text{g/mL}$  [9], and the use of the methanol extract of *Eleutherine americana* (L.) Merr tubers with the DPPH method also has a strong total antioxidant capacity and ferric reducing power with an  $IC_{50}$  value of  $16.95 \pm 1.58$   $\mu\text{g/mL}$  [10]. The naphthoquinone from *Eleutherine americana* (L.) Merr. was reported to modulate the prostaglandin pathway by inhibiting the COX-2 enzyme [11]. To evaluate the potency of bioactive compounds from *Eleutherine americana* (L.) Merr, we used the COX-2 receptor (PDB ID 5IKQ) with 2.41 Å resolution, and the results are supported by a 3D verification score of 90.93%. The receptor bound to meclufenamic acid as a native ligand with primary amino acid residues (SER530 and TYR385).

Theoretical investigation through in silico studies of bioactive compounds from *Eleutherine americana* (L.) Merr for COX-2 was explored by a previous study, but there is a lack of advanced information on dynamic properties and electronic parameters. A study providing deep mechanistic insight is needed by analyzing the dynamic stability and electronic properties using the DFT approach. The advanced computing technology in chemistry and pharmacy has enabled in silico analysis to evaluate ligand interactions with target proteins. In addition, the result can serve as a reference for future researchers before conducting experimental tests, reducing the risk of failure and opening new opportunities for developing Dayak onion-based phytopharmaceuticals in pharmacy, particularly for discovering anti-inflammatory drug candidates.

## 2. Experimental

### 2.1. Lipinski's Rules of Five and ADMET Studies

Lipinski's Rule of Five evaluates the drug properties of bioactive compounds from *Eleutherine americana* (L.) Merr before further in silico testing. This analysis aimed to assess whether the human body's mechanisms are

likely to absorb the compounds. Lipinski's Rule emphasizes that a compound is ideal for oral use if it has a molecular weight  $\leq 500$  Da, a hydrogen bond donor count  $\leq 5$ , a hydrogen bond acceptor count  $\leq 10$ , and an MlogP value between  $\leq 5$  [12]. The test was conducted via the website <https://scfbio-iitd.res.in/software/drugdesign/lipinski.jsp> (accessed on 17 September 2025), where each target compound that meets Lipinski's rules is considered more likely to be a safe and effective oral drug candidate.

### 2.2. Protein-ligand Interaction Network

Protein-ligand interaction network analysis was performed using the Search Tool for Interactions of Chemicals (STITCH) platform, accessible at <http://stitch.embl.de> by entering the name of the compound *Eleutherine americana* (L.) Merr. The target organism was set to Homo sapiens to validate biological relevance to human COX-2. The interaction confidence score was set at  $\geq 0.700$  with a high level of uncertainty. This system provides bioinformatics prediction data, literature development, and information about the affinity of protein networks with the compound *Eleutherine americana* L. Merr in various biological networks [13].

### 2.3. Molecular Docking Calculation

Molecular docking was used to calculate the interaction between the bioactive compound *Eleutherine americana* (L.) Merr and the target enzyme (COX-2). The initial docking stage involved preparing the target protein from the PDB database (ID 5IKQ), which could be downloaded in .pdb format from <https://www.rcsb.org/>. Before docking, the compound was optimized using the MMFF94 method to obtain the most stable structural conformation [14]. Next, it was prepared using Chimera 1.19 software to remove water molecules and add polar hydrogen atoms using Gasteiger charges. The redocking method was verified using meclufenamic acid as the native ligand, yielding a Root Mean Square Deviation (RMSD) of 0.45 Å. Meclufenamic acid is an NSAID that has anti-inflammatory activity by inhibiting the COX-2 enzyme. In addition, meclufenamic acid has been approved by the US FDA for the treatment of pain and inflammation [15].

The docking process was performed using AutoDockTools-1.5.6, which was capable of predicting the bond energy between ligands and proteins using a grid box that had been determined according to the location of the COX-2 enzyme active site, namely  $64 \times 64 \times 64$  with a grid distance of 0.375 Å relative to the centre coordinates (x: 22.023, y: 51.567, z: 17.649) using Lamarckian GA-4.2. The docking results were evaluated based on the lowest bond energy value and the type of bond interaction, such as hydrogen bonds or hydrophobic interactions. The docking complex was visualized using Biovia Discovery Studio to see the amino acid residues in the orientation of the ligand in the active site of the protein [16].

## 2.4. Prediction Study of ADMET

Absorption, Distribution, Metabolism, Excretion, and Toxicity (ADMET) analysis was used to predict pharmacokinetic properties, assess compound stability in the body, and minimize potential side effects of the drug candidate *Eleutherine americana* (L.) Merr through <https://admetmesh.scbdd.com/service/evaluation/index> (accessed on July 23, 2025) to explore the potential of the bioactive compound *Eleutherine americana* (L.) Merr as a safer and more effective COX-2 inhibitor for further development [17].

The standards used in absorption prediction include an ideal logP value between 0-5, TPSA <140 Å<sup>2</sup> for good oral absorption, and HIA 0-0.3 indicating good and effective absorption. Meanwhile, plasma protein binding can be considered safe if PPB >90%. Metabolism is assessed based on the potential for CYP enzyme inhibition; compounds that do not inhibit CYP3A4, CYP2D6, or CYP2C9 are considered to have a lower risk of metabolic interactions. Clearance indicates stable elimination without excessive accumulation, while toxicity in candidate compounds that are negative in the Ames test and do not inhibit the hERG channel are categorized as having low toxic risk. The application of the ADMET method enables the systematic early screening of drug candidates and increases the chances of successful development of bioactive compounds [18].

## 2.5. Density Functional Theory

Density Functional Theory (DFT) was used to predict the electronic properties of *Eleutherine americana* L. Merr, which is used as a candidate anti-inflammatory drug based on electron density, enabling accurate analysis of structure, stability, and chemical reactivity using the B3LYP 6-31G basis set theory to describe orbital shapes with Avogadro ORCA 4.1 and IboView v20150427 software. The geometric optimization process will produce minimum-energy structures, including the HOMO, LUMO, and energy gap, to evaluate the molecule's stability and potential reactivity. Orbital isosurface was visualized at a density value of 0.08 [19].

## 2.6. Molecular Dynamics Simulation

Molecular dynamics simulations were used to validate the stability of the ligand-protein complexes generated by docking. The complexes of eleutherine, isoeleutherine, and elecanacin with the COX-2 receptor were subjected to MD simulation using YASARA Structure version 25.1.13. The system parameters were set to physiological pressure, temperature, and pH (1 atm, 310K, and 7.4), and counter ions were Na<sup>+</sup> and Cl<sup>-</sup>. The MD simulation was performed using the AMBER 14 force field for 100 ns. The trajectory simulations were collected every 25 ps for further analysis in H<sub>2</sub>O solvent. Analysis of the trajectory to obtain RMSD of C<sub>α</sub>, RMSD of ligand configuration, Radius of Gyration (R<sub>G</sub>), total hydrogen bonds, and RMSF. The molecular mechanics Poisson-Boltzmann surface area (MM-PBSA) was used to estimate protein-ligand binding affinities, with high correlation with experimental data, as shown in Equation (1) [20].

$$MM - PBSA \text{ energy} = (E_{pot}^{Recep} + E_{solv}^{Recep} + E_{pot}^{Ligand} + E_{solv}^{Ligand}) - (E_{pot}^{Complex} + E_{solv}^{Complex}) \quad (1)$$

## 3. Results and Discussion

### 3.1. Lipinski's Rules of Five Studies

Physicochemical analysis was used to assess the suitability of a compound as an oral medication candidate, particularly in relation to Lipinski's rules and the golden triangle concept. Lipinski's rules emphasize that a compound ideal for oral use should have a molecular weight of less than 500 Da, fewer than 5 hydrogen bond donors, fewer than 10 hydrogen bond acceptors, and a logP value between 0 and 5 [21]. Based on the prediction results in Table 1, two compounds from *Eleutherine americana* (L.) Merr., namely Eleuthoside B and Eleuthoside C, violated Lipinski's rules because they have molecular weights >500 Da and >10 hydrogen bond acceptors. These properties may hinder membrane permeability and limit drug distribution across cell membranes [20]. Seventeen compounds from *Eleutherine americana* (L.) Merr meets the criteria that support the absorption and distribution processes in the body [22].

Furthermore, meclofenamic acid largely complies with Lipinski's rules but violates the HBA criterion, with a value of 14, which may worsen its oral bioavailability and increase toxicity risk, especially with long-term or high-dose use. However, it remains in clinical use due to well-established pharmacokinetic and safety data. Overall, from a physicochemical perspective, compounds from *Eleutherine americana* (L.) Merr appeared safer than the original meclofenamic acid ligand, showing a balanced polarity and lipophilicity that support membrane transport while maintaining adequate plasma solubility [23]. Compounds from *Eleutherine americana* (L.) Merr that satisfied all five Lipinski's rules were evaluated by molecular docking (Table 3). The results showed that eleutherine, isoeleutherine, and elecanacin had the lowest binding energies. These three compounds were further analyzed using ADMET predictions to assess their pharmacokinetic properties.

### 3.2. Protein-ligand Interaction Network

The Search Tool for Interacting Chemicals (STITCH) is used to predict interactions between *Eleutherine americana* (L.) Merr compounds and proteins based on literature data and computational predictions. This enables the identification of molecular networks that explain the functional relationship of a compound to its biological target [13]. Based on Figure 1, meclofenamic acid shows strong interactions with the inflammatory enzymes PTGS2 (COX-2) and PTGS1 (COX-1), with scores of 0.994 and 0.978, respectively [24]. Both enzymes play a role in prostaglandin biosynthesis, which triggers inflammation, pain, and fever, so inhibiting their activity explains the mechanism of action of meclofenamic acid as an NSAID. In addition, interactions with ALOX5 and AKR1C3 suggest an additional role in regulating leukotriene and steroid metabolism, while CNR1, ADIPOQ, and EDN1 are involved in regulating vasodilation, insulin sensitivity, and pain signal transmission.

**Table 1.** Lipinski's rule of five test for bioactive compounds from *Eleutherine americana* (L.) Merr

No.	Compounds	Lipinski's Rule of Five					Violation	Druglike
		Molecular Mass <500 (DA)	Log P <5	Hydrogen Bond Acceptor (HBA) <10	Hydrogen Bond Donor (HBD) <5			
1.	Native ligand ( <i>Meclofenamic acid</i> )	295.020	3.859	14	5	1	Unviolate	
2.	Eleuthoside A	406.130	0.933	9	4	0	Unviolate	
3.	Eleuthoside B	568.180	0.108	14	7	2	Violate	
4.	Eleuthoside C	598.230	0.440	14	8	2	Violate	
5.	Eleutherinoside A	418.130	1.310	4	0	0	Unviolate	
6.	Eleutherin	272.100	2.611	4	0	0	Unviolate	
7.	Eleutherol	244.070	3.228	4	1	0	Unviolate	
8.	Elecanacin	272.100	1.858	4	0	0	Unviolate	
9.	Isoeleutherin	272.100	2.703	4	0	0	Unviolate	
10.	1,3,6-trihidroxy-8-methyl-anthraquinone	270.050	3.359	5	3	0	Unviolate	
11.	Isoeleutherol	244.070	2.861	4	1	0	Unviolate	
12.	Erythrolaccin	286.050	3.393	6	4	0	Unviolate	
13.	Hongconin	288.100	3.211	5	2	0	Unviolate	
14.	1,5-dihidroxy-3-methylanthraquinone	254.060	4.170	4	2	0	Unviolate	
15.	Dihydroeleutherinol	258.090	3.453	4	2	0	Unviolate	
16.	Kadsurid Acid	470.340	7.012	4	2	1	Unviolate	
17.	Beta Sitosterol	414.390	8.025	1	1	1	Unviolate	
18.	2-acetyl-3,6,8-trihidroxy-1-methylanthraquinon	312.060	3.793	6	3	0	Unviolate	
19.	9-methoxy-1,3-dimethyl-3,4-dihydro-1H-benzo [9] isochromen e-5,10-dione	272.100	2.471	4	0	0	Unviolate	
20.	Naphthoquinone	158.040	1.625	2	0	0	Unviolate	

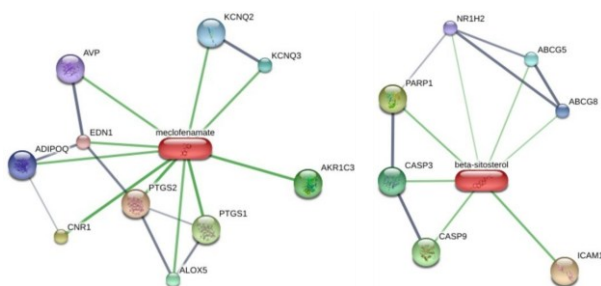


**Figure 1.** Protein-ligand interaction network using STITCH (a) meclofenamic acid (b) beta sitosterol

Meanwhile, beta-sitosterol, one of the main phytosterol compounds contained in *Eleutherine americana* (L.) Merr, interacts with the proteins CASP3, CASP9, PARP1, ICAM1, ABCG5, ABCG8, and NR1H2. These interactions indicate the ability of  $\beta$ -sitosterol compounds to induce intrinsic apoptosis, repair DNA, suppress oxidative stress, and regulate cholesterol homeostasis [25]. This suggests potential anticancer, anti-inflammatory, and hypocholesterolemic activities relevant to the pharmacological effects of *Eleutherine americana* (L.) Merr. Meanwhile, other compounds in

*Eleutherine americana* (L.) Merr are predicted to have not been extensively studied, thus requiring further research.

### 3.3. Molecular Docking Calculation

Molecular docking calculations are a form of structure-based drug design approach used to determine the interaction between drug candidate compounds and receptors through binding energy calculations and prediction of binding sites on the active side of enzymes combining several algorithms, such as genetic algorithms, simulated annealing, and incremental construction, which can adjust the conformation between the ligand and receptor until it reaches a minimum and stable free energy state [26]. Thus, binding energy, hydrogen bonds, and amino acid residues can be obtained and used as an initial description of the ligand's affinity for the receptor and the non-covalent interactions that stabilize the complex. Hydrogen bonds and van der Waals energy are recorded as the dominant contributors to the stability of the complex, followed by electrostatic interactions, while the polar and nonpolar energy of the solvent is also taken into account to obtain a more representative estimate of the total free energy [27].

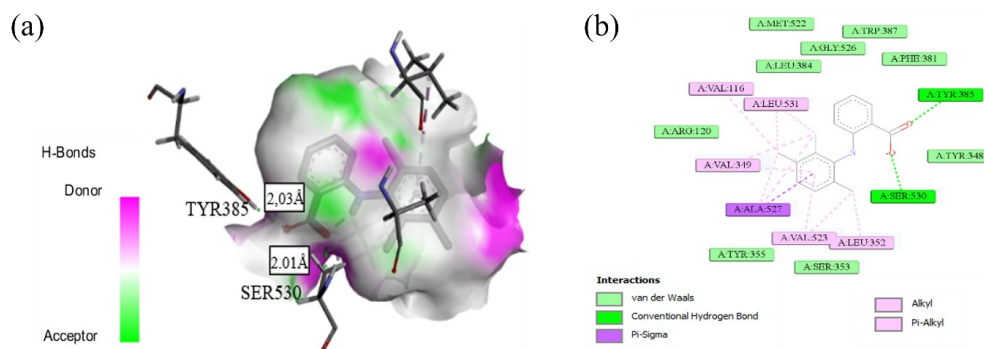


**Figure 2.** (a) 3D docking complex of meclufenamic acid ligand (b) 2D docking complex of meclufenamic acid ligand

The binding energy produced from the docking calculation is generally negative, indicating that the binding process occurs spontaneously. The more negative the binding energy value, the stronger the ligand's affinity in occupying the receptor's active site, thus increasing the potential of the ligand as an enzyme inhibitor [28]. The native ligand is used as a comparison because it has been shown to bind the receptor under physiological conditions. Thus, the native ligand's binding energy value becomes a reference for assessing whether the test compound has better binding affinity.

In this study, molecular docking calculations were performed between compounds from Dayak onion and the 5IKQ receptor as a representation of the COX-2 enzyme due to its role in regulating pain caused by inflammation, which is an unacceptable response for humans. In addition, the COX-2 enzyme is one of the four central mediators in inflammation that can regulate and maintain the inflammatory process, both acute and chronic [29]. The four central mediators in the inflammatory process include pro-inflammatory cytokines, chemokines, eicosanoids, and Reactive Oxygen Species (ROS). These mediators activate immune cells and regulate the inflammatory response, catalyze the formation of prostaglandins from arachidonic acid, and play a role in destroying pathogens. However, they can damage body tissue at high levels [30].

The native ligand meclufenamic acid exhibited a bond energy of  $-8.72$  kcal/mol, indicating a strong binding affinity to the COX-2 receptor with an RMSD of  $0.45$  Å and hydrogen bond interactions at SER530 and TYR385 [29]. Meanwhile, all compounds from *Eleutherine americana* (L.) Merr had a negative binding energy, indicating that the binding process was spontaneous and that the complexes formed were relatively stable. However, the binding energy of the compound from *Eleutherine americana* (L.) Merr was more positive compared to that of the native ligand. The colors on the protein surface that play a role in the ligand binding process (Figures 2, 3, 4, and 5). Green indicated the presence of hydrophobic residues that contribute to nonpolar interactions and support complex stabilization, where atom groups provide as hydrogen-bonding donors. At the same time, magenta represented atom acceptors that receive hydrogen with polar or charged properties that enable the formation of hydrogen bonds and electrostatic interactions.

Meanwhile, the white area functions as a transition zone with intermediate properties between polar and nonpolar, which plays a role in accommodating binding flexibility [31]. However, two compounds have energy values close to those of the native ligand, namely eleutherin ( $-8.09$  kcal/mol), isoeleutherin ( $-8.19$  kcal/mol), and elecanacin ( $-8.06$  kcal/mol). This means the compounds were still considered promising inhibitors [32]. The more negative the bond energy value, the greater the potential of the drug candidate compound as an inhibitor of the inflammatory COX-2 enzyme [33]. Meclufenamic acid has a bond energy of  $-8.72$  kcal/mol, higher than eleutherin  $-8.09$  kcal/mol which forms conventional hydrogen bonds between the carbonyl group of eleutherin and the SER530 residue at a distance of  $2.02$  Å and SER353 at a distance of  $2.10$  Å, which is within the optimal range for hydrogen bonds of  $1.5$ – $3.5$  Å, indicating a strong and directed interaction. In addition, the aromatic ring of eleutherin participates in a Pi-Pi T-shaped interaction with the TYR387 residue, which contributes to the stability of the ligand orientation within the catalytic pocket. Furthermore, hydrophobic contacts with residues VAL349 and LEU352 help strengthen ligand binding through nonpolar forces, resembling the interaction pattern of the control ligand meclufenamic acid.

The isoeleutherin compound exhibits the lowest bond energy among the test compounds at  $-8.19$  kcal/mol, indicating a highly competitive affinity for COX-2. Three main interaction motifs were identified: the strongest hydrogen bond formed between the ligand hydroxyl group and the catalytic residue SER530 at a distance of  $2.24$  Å, followed by additional hydrogen bonds with VAL523 at a distance of  $2.42$  Å and SER353 at a distance of  $2.96$  Å, which collectively stabilize the ligand position in the active site. In addition, the aromatic ring of isoeleutherine forms a Pi-Pi T-shaped interaction with TRP387, which is known to play an important role in COX-2 inhibitor binding. Additional hydrophobic interactions between LEU352 and VAL349 further strengthen the complex's stability through van der Waals interactions.

Meanwhile, elecanacin exhibits a binding energy of  $-8.06$  kcal/mol and interacts stably on the active site of COX-2 through a dominant hydrophobic motif. This compound forms a conventional hydrogen bond with the ALA527 residue, which functions as the initial anchor for

the ligand within the binding pocket. Other major interactions are hydrophobic and Pi-alkyl contacts with the VAL349, LEU352, and TYR355 residues, with an interaction distance of approximately 4.80 Å, which is still within the optimal range for hydrophobic interactions  $\leq 5.0$  Å. Additionally, the presence of aromatic residues TRP387 and TYR385 around the ligand provides additional stabilization through  $\pi$ -hydrophobic interactions, which favor the ligand's orientation during binding.

Visualization of the COX-2 binding pocket surface was performed using BIOVIA Discovery Studio 2021 Client with the Molecular-Receptor-Ligand Surface Interaction scheme. In this scheme, green represents hydrophobic/nonpolar areas that contribute to van der Waals and Pi-alkyl interactions, magenta indicates polar, charged areas or hydrogen bond acceptors, while white depicts neutral or transition zones with mixed polar and nonpolar properties [34]. A 3D analysis of the native ligand concerning the ligand-protein interaction showed two strong hydrogen bonds. The first bond was formed between the hydroxyl group of the amino acid residue TYR385 and the carbonyl group of the ligand. The second bond occurred between the hydroxyl group of SER530 and another carbonyl group. The interaction distances of 2.03 Å and 2.01 Å, indicated by the green dotted lines, fall

within the ideal range for hydrogen bonds (1.5–3.5 Å), indicating their high strength and stability [35].

Furthermore, the 3D visualization of the eleutherin compound showed that it formed two hydrogen bonds with the SER353 (2.10 Å) and SER530 (2.02 Å) residues in the protein's active site. These two residues were important in the enzyme's catalytic activity [36]. The carbonyl group in the compound acted as a strong hydrogen-bond acceptor, with the electronegative oxygen atom attracting hydrogen atoms from nearby target residues in a directed orientation, thereby helping to lock the ligand in position within the active site. This interaction increased the binding strength and enhanced the compound's ability to compete with natural substrates [37]. Furthermore, the aromatic ring in the compound exhibits Pi-Pi T-shaped interactions with the aromatic residue TYR387, as well as Pi-alkyl interactions with hydrophobic residues such as TYR348 and VAL523, providing additional stabilization energy [38]. The conformational fit between the ligand surface and the binding pocket also plays a role in maintaining the optimal orientation of the ligand. The combination of hydrogen interactions, aromatic and hydrophobic interactions, and the involvement of key amino acid residues in the catalytic pocket indicates that eleutherin has a high binding affinity, making it a potent enzyme inhibitor and therapeutic agent candidate [17].

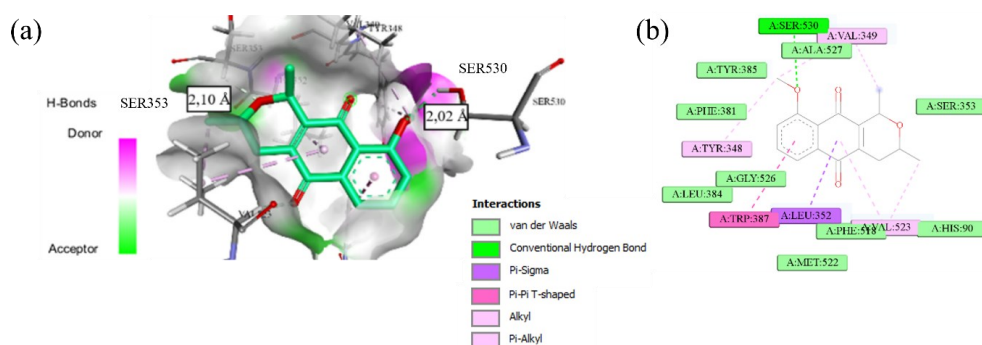


Figure 3. (a) Eleutherin ligand docking complex in 3D (b) Eleutherin ligand docking complex in 2D

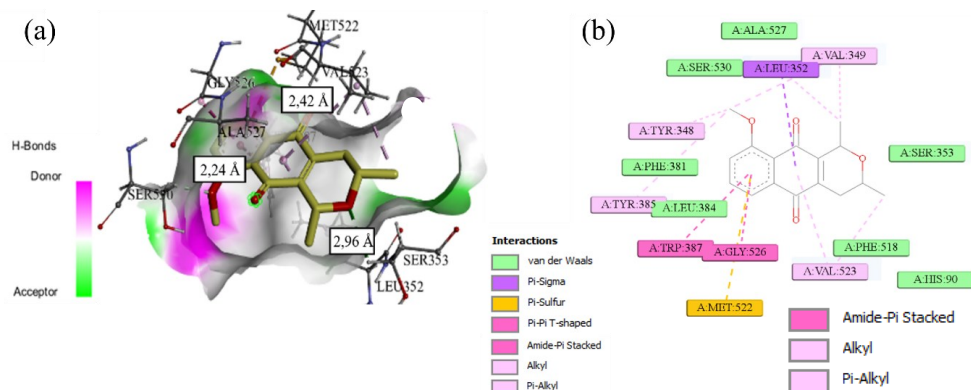
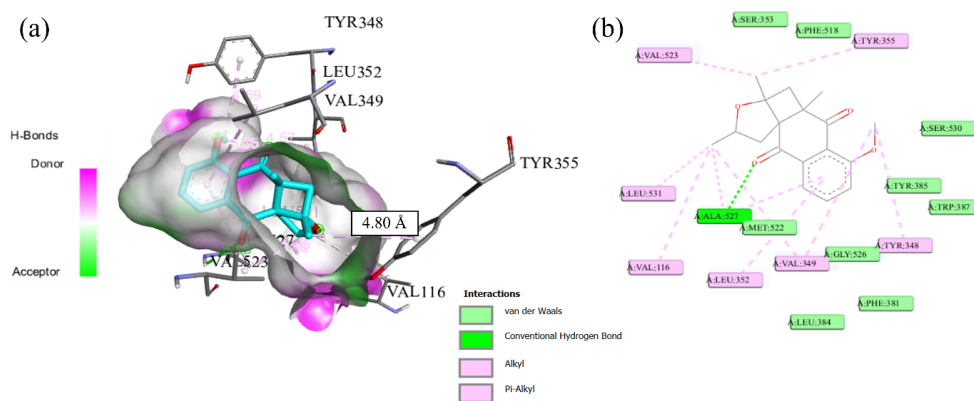


Figure 4. (a) Isoeleutherin 3D ligand docking complex (b) Isoeleutherin 2D ligand docking complex



**Figure 5.** (a) Elecanacin 3D ligand docking complex (b) Elecanacin 2D ligand docking complex

In addition, three hydrogen bonds were found in the isoeleutherin compound, which also stabilized the position of the ligand in the binding pocket. The strongest bond occurred between the ligand hydroxyl group and the carbonyl group of the SER530 residue with a length of 2.24 Å. The second bond formed between the ligand carbonyl oxygen and the amine group of VAL523 had a length of 2.42 Å and remained within the stable hydrogen bond range. Meanwhile, the longest bond, 2.96 Å, occurs between the ligand group and the SER353 residue, which, although weaker, still contributed to the overall stability of the interaction. The presence of these three bonds, with varying strengths, synergistically supported the optimal ligand position in the binding pocket [35].

Figure 6 shows that Elecanacin interacts through a number of non-covalent forces with various amino acid residues around the active site, such as VAL116, VAL349, LEU352, TYR348, and a distance of 4.80 Å between the ligand group and the amino acid residue TYR355 as a Pi-alkyl or hydrophobic stacking interaction that contributes to the stability of the complex. This dominant hydrophobic interaction stabilizes the ligand's position within the active pocket, enabling an optimal binding orientation. Overall, the docking calculation results of the 18 compounds of *Eleutherine americana* (L.) Merr are presented in Table 2. These can be further analyzed using molecular dynamics simulations to assess the complex's stability and, using MM-PBSA, estimate the binding free energy more accurately.

### 3.4. Prediction Study of ADMET

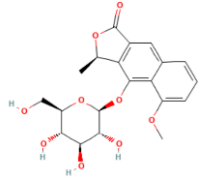
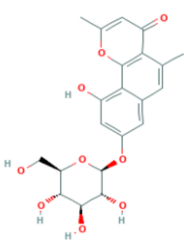
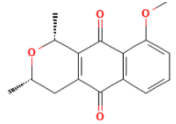
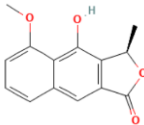
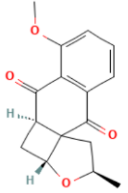
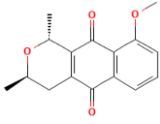
Based on the prediction results presented in Table 4, the absorption of the three compounds was predicted to have HIA values <0.3, indicating good intestinal absorption. Membrane permeability through the Caco-2 model also showed results close to  $-5.15 \log \text{ cm/s}$ , indicating fairly good penetration. However, eleutherin showed potent inhibition of P-glycoprotein transport, with a predictive value of +0.877, potentially inhibiting the absorption of other drugs and increasing the risk of drug interactions. At F20%, all four compounds remained within the ideal range, and at F30%, only isoeleutherin inhibited a high value of +0.999%, while meclofenamic acid, eleutherin, and had low predictive values <0.3%, indicating poor bioavailability [16, 39].

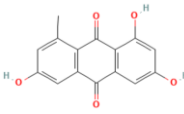
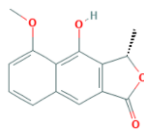
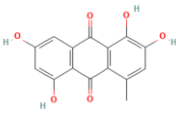
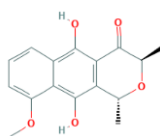
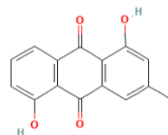
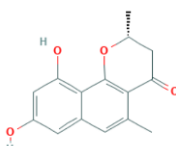
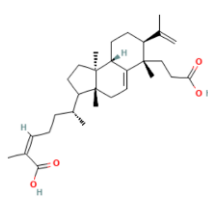
The distribution of compounds in the body was analyzed using PPB, VD, BBB, and Fu [40]. Three compounds were predicted to have PPB values above 90%, with meclofenamic acid reaching 99.281%, isoeleutherin 92.902%, and eleutherin 91.172%, indicating strong binding to plasma proteins. However, this is considered unfavorable pharmacologically due to the low Fu percentage. The penetration of the BBB by the three compounds indicated an excellent ability to penetrate the central nervous system, and the unbound fractions of meclofenamic acid, eleutherin, isoeleutherin, and elecanacin also revealed low values <5%, indicating that most of the molecules were in a bound form in plasma [41].

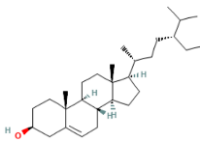
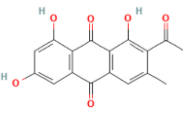
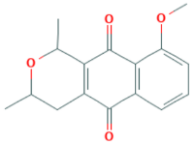
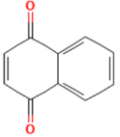
Metabolism was then evaluated, showing that all three compounds interacted with various CYP450 isoenzymes as substrates and inhibitors. Based on the metabolic prediction results, meclofenamic acid showed CYP1A2 substrate activity and CYP2C9 inhibitor activity. Based on the chemical characteristics of human biotransformation, the cytochrome P450 system comprises 57 isozymes that metabolize approximately two-thirds of all known drugs. Approximately 80% of these metabolic processes are catalyzed by five major isozymes: 1A2, 3A4, 2C9, 2C19, and 2D6. While eleutherine showed high activity against various isoenzymes, including CYP1A2, CYP2C19, and CYP3A4. This activity indicated that eleutherine has a complex metabolic profile and is prone to metabolic interactions with other compounds.

However, the isoeleutherin compound shows minimal interaction with these enzymes, thereby enhancing its metabolic stability. Regarding excretion, meclofenamic acid has a low clearance of 1,217 mL/min/kg, suggesting a slow elimination rate and potential accumulation in the body. In contrast, eleutherin and elecanacin show better clearance values, namely 6,743 and 7,472 mL/min/kg, respectively, and the half-life ( $t_{1/2}$ ) of these three compounds is less than 3 hours, indicating a reasonable elimination rate and supporting shorter dosing intervals [42]. Overall, the prediction results are shown in Table 3. Elecanacin shows favorable properties, followed by isoeleutherin, meclofenamic acid, and eleutherin, despite some mild indications; most parameters are within safe limits [43].

**Table 2.** Molecular docking calculations of the bioactive compound *Eleutherine americana* (L.) Merr against the COX-2 enzyme

No.	Compound	2D structure	PubChem ID	Binding energy (kcal/mol)	Amino acid residues	Ref.
1.	Native ligand (Meclofenamic acid)		4037	-8.72	Vdw: Met522; Leu384; Gly526; Trp387; Phe381; Tyr348; Ser353; Tyr355; Arg120 Conventional HBond: Tyr385; Ser530 Pi-Sigma: Ala527 Alkyl: Val523; Leu352; Leu531; Val116; Val349	[29]
2.	Eleuthoside A		274416316	-7.42	Vdw: Phe518; Leu352; Gly526; Trp387; Phe381; Tyr385; Tyr348; Val116; Arg120; Tyr355; Arg513; His90; Ser353 Conventional HBond: Val523; Ser530 Carbon HBond: Met522; Ala527 Pi-Alkyl: Val349; Leu531	[44]
3.	Eleutherinoside A		274670777	-3.41	Vdw: Val447; Tyr148; Phe210; Thr206; Gln203 Conventional HBond: His388; His214; Asn382; Tyr385 Unfavorable donor-Donor: Thr212 Pi-Donor Hydrogen Bond: Trp387 Pi-Pi Stacked: His386 Pi-Pi T-shaped: His207 Alkyl: Leu391 Pi-Alkyl: Ala202; Leu390	[7]
4.	Eleutherin		10166	-8.09	Vdw: Ala527; Ser353; His90; Phe518; Met522; Gly526; Leu384; Phe381; Tyr385 Conventional HBond: Ser530 Pi-Sigma: Leu352 Pi-Pi T-shaped: Tyr387 Alkyl: Val349 Pi-Alkyl: Tyr348; Val523	[45]
5.	Eleutherol		120697	-7.58	Vdw: Ser353; Val349; Tyr348; Leu352; Ser530; Phe381; Leu384; Trp387; Gly526; Phe518 Conventional HBond: Val523 Unfavorable Acceptor: Met522 Alkyl: Ala527 Pi-Alkyl: Tyr385	[46]
6.	Elecanacin		5491405	-8.06	Vdw: Ser353; Phe518; Ser530; Tyr385; Trp387; Gly526; Phe381; Leu384; Met522 Conventional HBond: Ala527 Alkyl: Leu531; Val116; Leu352; Val349; Tyr355 Pi-Alkyl: Tyr348; Val523	[7]
7.	Isoeleutherin		10445924	-8.19	Vdw: Ser530; Ala527; Ser353; His90; Phe518; Leu384; Phe381 Pi-Sigma: Leu352 Pi-Sulfur: Met522 Pi-Pi T-shaped: Trp387	[47]

No.	Compound	2D structure	PubChem ID	Binding energy (kcal/mol)	Amino acid residues	Ref.
					Amide-Pi Stacked: Gly526 Alkyl: Val349 Pi-Alkyl: Val523; Tyr348; Tyr385	
8.	1,3,6-trihidroxy-8-methyl-anthraquinone		12309204	-7.51	Vdw: Arg120; Ser353; His90; Ile517; Gln192; Phe518 Conventional HBond: Tyr355; Leu352; Ala527; Ser530 Pi-Sigma: Val349; Val523 Alkyl: Val116; Leu531	[7]
9.	Isoeleutherol		275139448	-7.28	Vdw: Gln203; Thr206; Asn382; His207; Val447; Leu391; Leu390 Conventional HBond: His388 Pi-Pi Stacked: His386 Alkyl: Tyr385 Pi-Alkyl: Ala202; Trp387; Phe210	[7]
10.	Erythrolaccin		9817337	-6.75	Vdw: Gln192; Ile517; Phe518; Leu534; Arg120; Ser353; His90 Conventional HBond: Ser530; Tyr355 Pi-Sigma: Val523; Val349; Ala527 Alkyl: Val116 Pi-Alkyl: Leu531	[11]
11.	Hongconin		274276047	-7.84	Vdw: Gln203; Thr206; Asn382; Thr212; Val447 Conventional HBond: Tyr385; His388 Pi-Sigma: Phe210; His207 Pi-Pi Stacked: His386 Alkyl: Leu390 Pi-Alkyl: Ala202; Trp387	[11]
12.	1,5-dihidroxy-3-methylantraquinone		5316800	-8.02	Vdw: Tyr385; Ser530; Ser353; Phe518; Phe381 Coventional HBond: Leu352 Carbon HBond: Gly526 Pi-Pi T-shaped: Trp387 Alkyl: Val349; Met522; Leu384 Pi-Alkyl: Tyr348; Val523	[7]
13.	Dihydroeleutherinol		102473740	-7.89	Vdw: Phe381; Tyr385; Ser530; Ser353; Phe518; Phe381 Conventional HBond: Leu352 Carbon HBond: Gly526 Pi-Pi T-shaped: Trp387 Alkyl: Val349; Met522; Leu384 Pi-Alkyl: Val348; Val523	[11]
14.	Kadsurid Acid		5384417	-7.9	Vdw: Tyr148; Thr212; Lys211; Phe210; His388; Leu294; Val295; Tyr404; Leu391; Asn382; Gln454 Conventional HBond: His214; Gln203 Pi-Sigma: His207 Alkyl: His386 Pi-Alkyl: Val444; Val447; Ile408	[7]

No.	Compound	2D structure	PubChem ID	Binding energy (kcal/mol)	Amino acid residues	Ref.
15.	Beta Sitosterol		222284	-7.87	Vdw: Tyr404; Asn382; Thr212; Gln203; Ala199; Trp387 Conventional HBond: His214 Alkyl: Leu391; Val447; Val444; Leu294; Leu390 Pi-Alkyl: His386; His207; His388	[7]
16.	2-acetyl-3,6,8-trihydroxy-1-methylantraquinon		12742404	-8.0	Vdw: Leu384; Trp387; Phe518; Arg120; Val116; Le359; Phe381; Tyr385 Conventional HBond: Gly526; Ser530 Carbon HBond: Ala527; Ser353 Pi-Sigma: Val523 Pi-Sulfur: Met522 Alkyl: Leu531 Pi-Alkyl: Val349; Leu352	[11]
17.	9-methoxy-1,3-dimethyl-3,4-dihydro-1H-benzo[9]isochromen e-5,10-dione		4483892	-8.0	Vdw: Ala199; Gln203; Thr206; Tyr385; His207; Asn382 Carbon HBond: His388 Pi-Donor HBond: Trp387 Pi-Sigma: Leu390 Alkyl: Leu391 Pi-Alkyl: His386; Phe210; Ala202	[11]
18.	Naphthoquinone		8530	-6.18	Vdw: Ala527; Val523; Phe518; Gly526; Leu384; Phe381; Ser530; Tyr348 Conventional HBond: Tyr385 Pi-Sigma: Leu352 Pi-Sulfur: Met522 Pi-Pi T-shaped: Trp387 Pi-Alkyl: Val349	[11]

### 3.5. Density Functional Theory

DFT is used to analyze electron density calculations. DFT enables the analysis of orbital energies such as the Highest Occupied Molecular Orbital (HOMO) and the Lowest Unoccupied Molecular Orbital (LUMO) to evaluate the stability and reactivity of a compound. The  $E_g$  value describes a molecule's chemical reactivity: a lower value indicates greater reactivity and a better ability to transfer electrons when interacting with biological targets. Based on the DFT calculation results shown in Table 4, the isoeleutherin compound has the lowest  $E_g$  value (3.467 eV) compared to the reference ligands meclofenamic acid (4.254 eV) and elecanacin (4.358 eV), indicating a higher level of electronic reactivity.

Isoeleutherine is known to have better electronic flexibility because its  $E_g$  value is lower than that of meclofenamate acid. This allows for more adaptive charge distribution when interacting with active enzyme residues. These conditions support more effective electron donor-acceptor behavior, particularly in hydrogen bond formation, where the ligand's HOMO orbital acts as an electron donor and the LUMO orbital acts as an acceptor to polar residues on the active site. In addition, the conjugated  $\pi$  system in isoeleutherine, with a smaller  $E_g$ , facilitates noncovalent interactions, such as

Pi-Pi stacking, with the aromatic residue TYR 385. Conversely, meclofenamate acid, with a larger  $E_g$  value, exhibits lower polarization and lower electronic response, so that donor-acceptor interactions and charge adjustment during the binding process tend to be less optimal. This result was in line with the molecular docking result: isoeleutherin had the lowest binding energy. Therefore, the distribution of delocalized HOMO orbitals on the aromatic ring and carbonyl group indicates the ability to act as an electron donor, while the distribution of LUMO orbitals indicates electron acceptor regions that enable effective interactions with amino acid residues such as SER530, SER353, and TYR385.

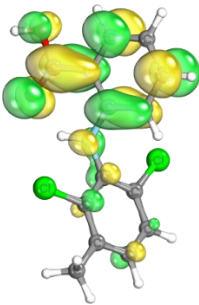
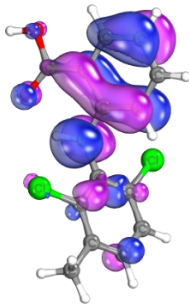
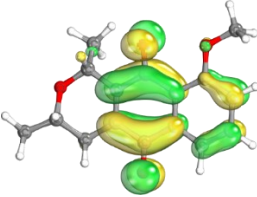
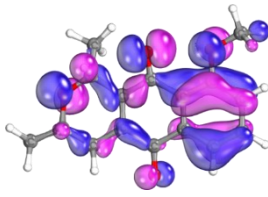
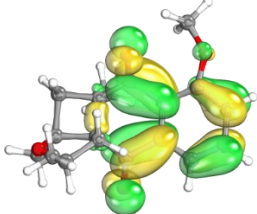
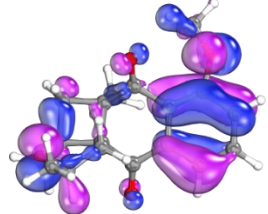
Orbital visualization shows different HOMO and LUMO electron distributions between compounds, where purple and blue areas indicate electron-rich regions, while yellow and red areas indicate electron-deficient regions. The delocalization of the HOMO and LUMO orbitals involving oxygen groups and aromatic structures indicates the potential for strong interactions with biological receptors through hydrogen bonds and Pi-Pi stacking forces. Thus, the smaller HOMO-LUMO energy gap in isoeleutherin correlates with higher binding energy in docking results, confirming that the electronic properties of molecules contribute to the stability and strength of ligand-protein complexes.

Table 3. ADMET prediction of *Eleutherine americana* (L.) Merr compounds

Parameters	Meclofenamic acid	Eleutherin	Isoeleutherin	Elecanacin
<b>Medical Chemistry</b>				
Lipinski Rule	Accepted	Accepted	Accepted	Accepted
Pfizer Rule	Rejected	Accepted	Accepted	Accepted
GSK Rule	Rejected	Accepted	Accepted	Accepted
Golden triangle	Accepted	Accepted	Accepted	Accepted
<b>Absorption</b>				
Human Intestinal Absorption (HIA) (%)	---0.003	---0.003	---0.014	---0.003
Permeability Caco-2 (log cm/s)	-4.472	-4.575	-4.570	-4.681
P-glycoprotein inhibitor	---0.001	++0.877	---0.011	---0.03
P-glycoprotein substrate	---0.002	---0.0	---0.009	---0.0
F20%	---0.001	---0.005	---0.005	---0.003
F30%	---0.01	-0.396	-0.49	---0.01
<b>Distribution</b>				
Plasma Protein Binding (PPB) (%)	99.281	91.172	92.902	85.196
Blood-Brain Barrier (BBB) (cm/s)	---0.133	---0.091	---0.062	--0.112
Volume Distribution (L/kg)	0.268	0.847	0.914	1.414
Fu (%)	0.843	2.028	1.521	7.658
<b>Metabolism</b>				
CYP1A2 inhibitor	+0.502	+++0.970	+++0.948	+0.627
CYP1A2 substrate	++0.872	++0.802	--0.247	++0.841
CYP2C19 inhibitor	--0.191	+++0.959	---0.074	+0.622
CYP2C19 substrate	--0.142	+++0.949	---0.052	++0.8
CYP2C9 inhibitor	+0.699	++0.827	+0.525	-0.336
CYP2C9 substrate	++0.711	--0.244	+0.663	-0.471
CYP2D6 inhibitor	--0.245	--0.233	-0.418	---0.024
CYP2D6 substrate	--0.115	--0.238	--0.203	++0.777
CYP3A4 inhibitor	--0.109	+0.564	++0.789	+0.655
CYP3A4 substrate	--0.132	--0.284	--0.115	-0.484
<b>Excretion</b>				
Half-time (t <sup>1/2</sup> )	0.536	0.110	0.098	0.166
Clearance	1.217	6.743	3.408	7.472
<b>Toxicity</b>				
Human Hepatotoxicity	++0.84	++0.737	---0.045	+0.663
hERG Blockers	---0.06	---0.019	---0.059	---0.077
Rat Oral Acute Toxicity	++0.751	+0.685	---0.088	-0.491
AMES Toxicity	---0.017	+++0.964	++0.768	++0.893
Drug-Induced Liver Injury	+++0.986	+++0.901	++0.88	++0.839
Carcinogenicity	-0.345	+++0.939	--0.207	-0.43
FDAMDD	--0.202	+++0.942	+++0.930	+++0.922
Skin Sensitization	+0.553	++0.844	+0.598	-0.396
Eye Corrosion	---0.004	---0.01	---0.004	---0.004
Eye Irritation	---0.078	++0.863	+++0.966	--0.202
Respiratory Toxicity	+++0.937	+++0.959	---0.085	++0.836

\* Symbols and probability values: 0-0.1 (---) very safe, 0.1-0.3 (--) safe, 0.3-0.5 (-) moderate, 0.5-0.7 (+) low toxic risk, 0.7-0.9 (++) moderate toxic risk, and 0.9-1.0 (+++) high toxic risk.

Table 4. DFT of *Eleutherine americana* (L.) Merr compounds

Compounds	LUMO	Representation	HOMO	Representation	Eg (eV)
Meclofenamic acid	-1.358 eV		-5.612 eV		4.254 eV
Isoeleutherin	-2.995 eV		-6.462 eV		3.467 eV
Elecanacin	-2.147 eV		-6.505 eV		4.358 eV

### 3.6. Molecular Dynamics Simulation

Molecular dynamics simulations were performed to observe the dynamic properties of the COX-2 enzyme complex with a drug candidate from Dayak onion at the atomic scale. The simulation was run for 100 ns using YASARA Structure software with the AMBER14 force field at a temperature of 310K to evaluate the stability of the ligand bond in the active pocket of COX-2, observe the flexibility of the protein structure, and calculate the binding energy of the ligand to the receptor [48]. The data obtained from simulations of eleutherin, isoeleutherin, and elecanacin were compared with those of the native ligand, meclofenamic acid. Molecular dynamics plays a role in analyzing ligand stability on the active side of the protein through several parameters, such as RMSD  $C_{\alpha}$ , RMSD, RMSF,  $R_G$ , MM-PBSA, and the number of hydrogen bonds formed during the simulation [20].

RMSD of  $C_{\alpha}$  atoms indicates macromolecular conformational changes and assesses protein structure stability during molecular dynamics simulations [49]. Figure 6A shows that the  $C_{\alpha}$  RMSD values for all complexes were below 3 Å, indicating the stabilization of proteins during the 100 ns simulation. At the beginning of the 0–20 ns simulation, there was a slight increase in the elecanacin compound with a  $C_{\alpha}$  RMSD value of 2.5 Å and meclofenamic acid 2.4–2.5 Å. After the equilibration phase, the three complexes showed small fluctuations without significant spikes, suggesting that ligand presence did not cause significant conformational changes in the protein structure, with an average of 2–2.5 Å [50]. Based on the average standard deviation values calculated over the last 20 ns of the simulation, the

complexes showed good stability, with a constant RMSD ( $C_{\alpha}$ ) < 3 Å. The average RMSD values were 1.47 Å for eleutherin, 1.87 Å for isoeleutherine, and 1.93 Å for elecanacin, reflecting the relatively stable position of the ligand in the active site of the protein.

In addition, the stable RMSD  $C_{\alpha}$  in the 1–3 Å range indicated that the ligands tested, meclofenamic acid, eleutherin, isoeleutherin, and elecanacin, did not cause instability in the protein. Complexes with consistent RMSD throughout the simulation indicate that ligand binding occurs without disrupting the protein fold [51]. Thus, these RMSD  $C_{\alpha}$  values reinforce the evidence that the system achieves stability under simulation conditions. Therefore, the compound *Eleutherine americana* (L.) Merr can maintain its binding pose in the active site of COX-2. The RMSD of the ligand configuration shown in Figure 6B indicates the stability of the ligand's position and orientation in the protein binding pocket during the simulation. Analysis of the ligand RMSD showed that the eleutherin complex remained stable over 100 ns, with a range of 0.4–1.2 Å.

However, the isoeleutherin ligand exhibited different dynamics from eleutherin and meclofenamic acid, where the stability from the start of the simulation was in the range of 1–1.4 Å. Despite these differences, eleutherin, isoeleutherin, and elecanacin still showed that the interaction of ligands with residues at the active site is strong enough that the ligands do not move significantly from their initial positions, and the orientation of hydrogen bonds [52], hydrophobic bonds, and electrostatic interactions can be maintained throughout the simulation [53].

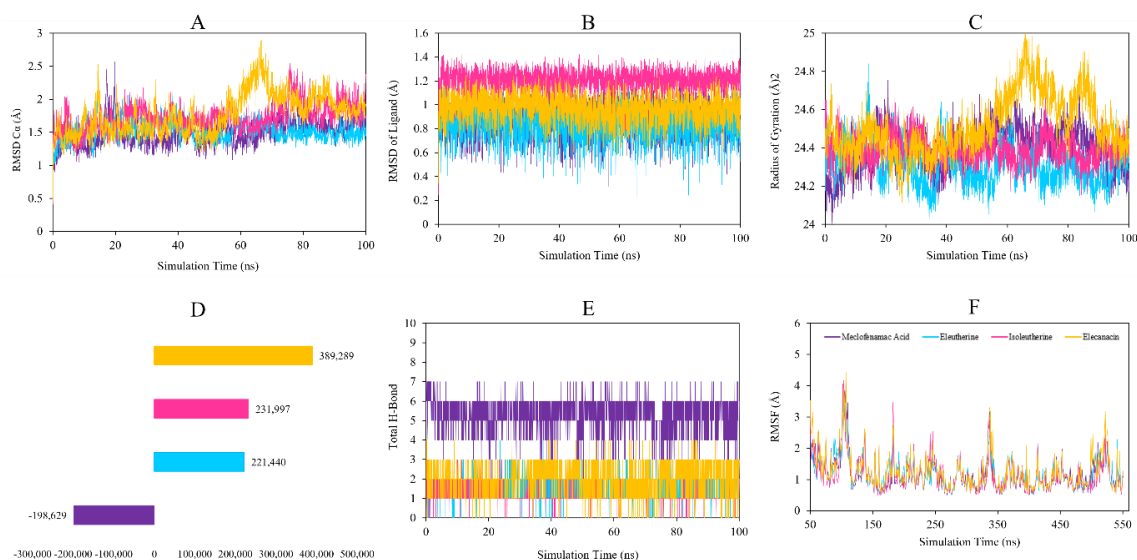


**Figure 6.** (A) RMSD C $\alpha$  of eleutherin, isoeleutherin, and eleanacin complexes with COX-2, (B) RMSD of ligand configuration, (C) Comparison of R<sub>G</sub> patterns between eleutherin, isoeleutherin, and eleanacin complexes against COX-2, (D) MM-PBSA of eleutherin, isoeleutherin, and eleanacin complexes against COX-2, (E) Total hydrogen bonds of eleutherin, isoeleutherin, and eleanacin against COX-2, (F) RMSF

Analysis of the radius of gyration (R<sub>G</sub>) describes the density and compactness of the protein structure throughout the simulation. The R<sub>G</sub> value can also indicate the dynamics of the test compounds and protein complexes concerning the solvent [54]. A stable R<sub>G</sub> value indicates that the protein does not exhibit significant conformational changes. Based on Figure 6C, the R<sub>G</sub> value was 24–24.8 Å for three complexes: meclofenamic acid, eleutherin, and isoeleutherin. However, this is different from eleanacin, which experienced fluctuations reaching 24.9 Å at 65 ns. It indicates that the protein fold is well maintained even in the presence of bound ligands. R<sub>G</sub> stability also supports the RMSD analysis, indicating that the presence of ligands does not cause structural destabilization [55]. A low R<sub>G</sub> value indicates that the protein is in a well-folded state, while a high value reflects a condition in which the protein is unfolded or has undergone structural expansion [54].

Next, the MM-PBSA analysis calculates the free energy of ligand binding to protein, used to evaluate the free energy contribution of the complex during simulation, and confirms the stability of the ligand interaction with the receptor [56]. MM-PBSA calculations revealed that the eleutherin, isoeleutherin, and eleanacin complexes had positive energy values. In the YASARA script convention, md\_analyzebindenergy.mcr calculates the relative interaction energy as the difference between the total potential energy and the solvation energy of separate protein-ligand complexes. The higher the positive value, the stronger the interaction between the protein and the ligand, and the greater the ligand's stability. Meanwhile, negative energy values indicate a weaker binding affinity [57]. Figure 6D shows that the highest relative interaction energies are possessed by eleanacin (389.289 kcal/mol), isoeleutherin (231.997 kcal/mol), and eleutherin (221.440 kcal/mol), respectively. Conversely, meclofenamic acid shows a lower and negative energy value (-198.629 kcal/mol) because this ligand is a native ligand that is crystallized

with the COX-2 protein and has been in a stable biological minimum energy configuration [58]. This tends to produce more negative energy values because optimal interactions between ligands and active protein residues have been established since the crystallization process. In addition, several factors such as hydrogen bond stability, hydrophobic interactions, and entropy contributions also influence the success of the bond [59].

Figure 6E shows the total number of hydrogen bonds that play a role in determining the stability and specificity of ligand binding to proteins. Meclofenamic acid has a higher average number of hydrogen bonds, reaching 5.366, compared to *Eleutherine americana* (L.) Merr compounds, namely eleutherin 1.677, isoeleutherin 1.184, and eleanacin 1.984. This condition aligns with higher bond energies, highlighting the role of hydrogen bonds as a major contributor to bond affinity. Meanwhile, eleutherin, isoeleutherin, and eleanacin showed fewer hydrogen bonds but remained relatively consistent throughout the simulation. This condition indicates that hydrogen interactions are fewer than in the original ligand; ligands from the compound *Eleutherine americana* (L.) Merr can still bond stably through other mechanisms, such as hydrophobic or van der Waals interactions [60].

RMSF analysis provides an overview of the flexibility level of each protein residue during the simulation process. As shown in Figure 6F, the fluctuation patterns are relatively similar in all four complexes, with several fluctuation peaks occurring in the polypeptide chain. RMSF below 3 Å indicates that the interaction between the ligand and the enzyme tends to be stable, while high RMSF values can cause deviations in RMSD values. The results for the eleutherin, isoeleutherin, and eleanacin complexes show that the RMSF of the COX-2 protein residues are mainly in the range of 2 to 4 Å. However, several residues showed RMSF values above 3 Å, even exceeding 4 Å, which indicated the possibility of bond relaxation in the conformation of the target protein. The

RMSF pattern between meclofenamic acid and eleutherin, isoeleutherin, and elecanacin exhibited that the *Eleutherine americana* (L.) Merr ligand did not cause significant changes to protein residue dynamics. This condition proved that ligand binding does not cause significant disturbances to protein flexibility but maintains a dynamic pattern similar to the control ligand [61].

#### 4. Conclusion

A study of bioactive compounds from *Eleutherine americana* (L.) Merr against the COX-2 enzyme has been successfully evaluated using Lipinski's rule of five, STITCH network analysis, molecular docking, ADMET properties, DFT analysis, and molecular dynamics. The docking evaluation stage of 18 compounds resulted in 3 compounds, namely eleutherin, isoeleutherin, and elecanacin, which met the drug suitability criteria for further analysis. The molecular docking results indicated that eleutherin, isoeleutherin, and elecanacin had relatively strong binding affinities and interacted with amino acid residues in the active site of COX-2, thus supporting the possibility of molecular inhibition of the prostaglandin formation pathway. Isoeleutherin was identified as the most promising compound as a potential theoretical anti-inflammatory mechanism as a COX-2 COX-2 (PTGS2) in PDB 5IKQ inhibitor with the lowest binding energy compared to other test compounds, namely (-8.19 kcal/mol), close to the control ligand meclofenamic acid (-8.72 kcal/mol), and forms interactions with key residues on the active site of COX-2, namely SER530, SER353, ALA527, HIS90, PHE518, LEU384, and PHE381, which play an important role in COX-2 inhibitor binding. The advantage of isoeleutherin is reinforced by density functional theory analysis, in which the compound exhibits the smallest HOMO-LUMO energy gap (3.467 eV) compared to the reference ligand and other test compounds. A smaller energy gap indicates higher electronic reactivity, thus theoretically supporting the ability of isoeleutherin to form and maintain non-covalent interactions with the active residues of COX-2. Further validation through molecular dynamics simulations for 100 ns showed that the isoeleutherin against the COX-2 complex remained structurally stable, with  $C_{\alpha}$  RMSD values below 3 Å and ligand RMSD in the range of 1.0-1.4 Å. RMSF patterns and radius of gyration comparable to the control ligand confirm that the docking orientation of isoeleutherin can be maintained under dynamic conditions resembling physiological conditions. Thus, based on the consistency of docking binding affinity results, electronic reactivity support from DFT analysis, and complex stability confirmed through MD simulation, isoeleutherin shows promising characteristics for development as a herbal-based COX-2 inhibitor candidate. These findings clearly demonstrate the potential of the bioactive compound *Eleutherine americana* (L.) Merr in inhibiting COX-2, so further in vitro and in vivo studies are still needed to validate its theoretical potential as a candidate herbal anti-inflammatory drug.

#### Acknowledgment

The authors thank The Ministry of Religious Affairs–The Awakened Indonesia Research Funds (MoRa The Air Funds) 2024 for providing the necessary facilities.

#### References

- [1] Daniela Placha, Josef Jampilek, Chronic Inflammatory Diseases, Anti-Inflammatory Agents and Their Delivery Nanosystems, *Pharmaceutics*, 13, 1, (2021), 64  
<https://doi.org/10.3390/pharmaceutics13010064>
- [2] Jean-Luc Wautier, Marie-Paule Wautier, Pro- and Anti-Inflammatory Prostaglandins and Cytokines in Humans: A Mini Review, *International Journal of Molecular Sciences*, 24, 11, (2023), 9647  
<https://doi.org/10.3390/ijms24119647>
- [3] Mohsen Ahmadi, Sander Bekeschus, Klaus-Dieter Weltmann, Thomas von Woedtke, Kristian Wende, Non-steroidal anti-inflammatory drugs: recent advances in the use of synthetic COX-2 inhibitors, *RSC Medicinal Chemistry*, 13, 5, (2022), 471-496  
<https://doi.org/10.1039/d1md00280e>
- [4] Zhiran Ju, Menglan Li, Junde Xu, Daniel C. Howell, Zhiyun Li, Fen-Er Chen, Recent development on COX-2 inhibitors as promising anti-inflammatory agents: The past 10 years, *Acta Pharmaceutica Sinica B*, 12, 6, (2022), 2790-2807  
<https://doi.org/10.1016/j.apsb.2022.01.002>
- [5] Jaya Prabhakaran, Andrei Molotkov, Akiva Mintz, J. John Mann, Progress in PET Imaging of Neuroinflammation Targeting COX-2 Enzyme, *Molecules*, 26, 11, (2021), 3208  
<https://doi.org/10.3390/molecules26113208>
- [6] Rahmi Annisa, Mochammad Yuwono, Esti Hendradi, Effect of vegetable oil on self-nanoemulsifying drug delivery system of Dayak Onion (*Eleutherine palmifolia* (L.) Merr.) extract using hydrophilic-lipophilic balance approach: formulation, characterization, *International Journal of Drug Delivery Technology*, 10, 2, (2020), 210-216  
<https://doi.org/10.25258/ijddt.10.2.4>
- [7] Mokhamat Ariefin, Rizki Rachmad Saputra, Study Natural Compound of *Eleutherine americana* as a SaR-CoV-2 Therapeutic Agent : In Silico Approach, *ALCHEMY: Journal of Chemistry*, 11, 1, (2023), 41-49  
<https://doi.org/10.18860/al.v11i1.18018>
- [8] Roji Septian Hardi, Slamet Slamet, Laila Kamilla, Uji aktivitas anti inflamasi ekstrak bawang dayak (*Eleutherine americana* L. Merr) terhadap stabilisasi membran sel darah merah, *Jurnal Laboratorium Khatulistiwa*, 2, 1, (2019), 30-36  
<https://doi.org/10.30602/jlk.v2i1.324>
- [9] Oktariani Pramiastuti, Devi Ika Kurnianingtyas Solikhati, Aprilia Suryani, Aktivitas Antioksidan Fraksi Umbi Bawang Dayak (*Eleutherine bulbosa* (Mill.) Urb) dengan Metode DPPH (1, 1-difenil-2-pikrilhidrazil), *Jurnal Wiyata: Penelitian Sains dan Kesehatan*, 8, 1, (2021), 55-66
- [10] Farida Laila, Ika Resmeliana, Wina Yulianti, Atep Dian Supardan, Evaluasi Kadar Senyawa Fenolat, Flavonoid Total, serta Aktivitas Antioksidan Secara in vitro dalam Ekstrak Metanol Bawang Dayak (*Eleutherine palmifolia* (L.) Merr), *Kovalen: Jurnal Riset Kimia*, 8, 3, (2022), 298-307

- [11] Muhamad Insanu, Siti Kuswardiyani, Rika Hartati, Recent Studies on Phytochemicals and Pharmacological Effects of *Eleutherine Americana* Merr, *Procedia Chemistry*, 13, (2014), 221-228 <https://doi.org/10.1016/j.proche.2014.12.032>
- [12] James H. McKerrow, Christopher A. Lipinski, The rule of five should not impede anti-parasitic drug development, *International Journal for Parasitology: Drugs and Drug Resistance*, 7, 2, (2017), 248-249 <https://doi.org/10.1016/j.ijpddr.2017.05.003>
- [13] Damian Szklarczyk, Alberto Santos, Christian von Mering, Lars Juhl Jensen, Peer Bork, Michael Kuhn, STITCH 5: augmenting protein-chemical interaction networks with tissue and affinity data, *Nucleic Acids Research*, 44, D1, (2015), D380-D384 <https://doi.org/10.1093/nar/gkv1277>
- [14] Permono Adi Putro, Desi Wulandari, Devia Putri Wulandari, Fitriah Nurfaidah, M Farid Ahdan, Seviana Chaerunnisa, Vina Umay Octaviani, A Force Field Simulation Approach to Analyze the Molecular Structure Stability of Cyanidin-3-Glucoside Using Avogadro: A Preliminary Study, *TIME in Physics*, 2, 2, (2024), 66-76 <https://doi.org/10.11594/timeinphys.2024.v2i2p66-76>
- [15] Stephanie Hopkins, Victor Yang, David F. L. Liew, Choosing a nonsteroidal anti-inflammatory drug for pain, *Australian Prescriber*, 48, 4, (2025), 139 <https://doi.org/10.18773/austprescr.2025.032>
- [16] Leonardo G. Ferreira, Ricardo N. Dos Santos, Glaucius Oliva, Adriano D. Andricopulo, Molecular Docking and Structure-Based Drug Design Strategies, *Molecules*, 20, 7, (2015), 13384-13421 <https://doi.org/10.3390/molecules200713384>
- [17] Leonardo L. G. Ferreira, Adriano D. Andricopulo, ADMET modeling approaches in drug discovery, *Drug Discovery Today*, 24, 5, (2019), 1157-1165 <https://doi.org/10.1016/j.drudis.2019.03.015>
- [18] Imad Ahmad, Aleksey E. Kuznetsov, Abdul Saboor Pirzada, Khalaf F. Alsharif, Maria Daglia, Haroon Khan, Computational pharmacology and computational chemistry of 4-hydroxyisoleucine: Physicochemical, pharmacokinetic, and DFT-based approaches, *Frontiers in Chemistry*, Volume 11 - 2023, (2023), <https://doi.org/10.3389/fchem.2023.1145974>
- [19] Mohamed Hagar, Hoda A. Ahmed, Ghadah Aljohani, Omaira A. Alhaddad, Investigation of Some Antiviral N-Heterocycles as COVID 19 Drug: Molecular Docking and DFT Calculations, *International Journal of Molecular Sciences*, 21, 11, (2020), 3922 <https://doi.org/10.3390/ijms21113922>
- [20] Wiji Utami, Apriyanto Apriyanto, Laila Antari, Herlina Rasyid, Ika Nur Fitriani, Inhibition of Human Acetylcholinesterase (4EY7) using Bioactive Compound from *Moringa oleifera*: Molecular Docking and Dynamic Studies, *Jurnal Kimia Valensi*, 10, 2, (2024), 290-303 <https://doi.org/10.15408/jkv.v10i2.39840>
- [21] Thomas K. Karami, Shumet Hailu, Shaoxin Feng, Richard Graham, Hovhannes J. Gukasyan, Eyes on Lipinski's Rule of Five: A New "Rule of Thumb" for Physicochemical Design Space of Ophthalmic Drugs, *Journal of Ocular Pharmacology and Therapeutics*, 38, 1, (2022), 43-55 <https://doi.org/10.1089/jop.2021.0069>
- [22] Mamaru Bitew, Tegene Desalegn, Taye B. Demissie, Anteneh Belayneh, Milkyas Endale, Rajalakshmanan Eswaramoorthy, Pharmacokinetics and drug-likeness of antidiabetic flavonoids: Molecular docking and DFT study, *PLoS ONE*, 16, 12, (2021), e0260853 <https://doi.org/10.1371/journal.pone.0260853>
- [23] Alina Pyka-Pająk, Wioletta Parys, Małgorzata Dołowy, Comparison of the Utility of RP-TLC Technique and Different Computational Methods to Assess the Lipophilicity of Selected Antiparasitic, Antihypertensive, and Anti-inflammatory Drugs, *Molecules*, 24, 17, (2019), 3187 <https://doi.org/10.3390/molecules24173187>
- [24] Michael Kuhn, Damian Szklarczyk, Andrea Franceschini, Monica Campillos, Christian von Mering, Lars Juhl Jensen, Andreas Beyer, Peer Bork, STITCH 2: an interaction network database for small molecules and proteins, *Nucleic Acids Research*, 38, suppl\_1, (2009), D552-D556 <https://doi.org/10.1093/nar/gkp937>
- [25] Haoyu Wang, Zhi Wang, Zihui Zhang, Jingchun Liu, Li Hong,  $\beta$ -Sitosterol as a Promising Anticancer Agent for Chemoprevention and Chemotherapy: Mechanisms of Action and Future Prospects, *Advances in Nutrition*, 14, 5, (2023), 1085-1110 <https://doi.org/10.1016/j.advnut.2023.05.013>
- [26] Jiyu Fan, Ailing Fu, Le Zhang, Progress in molecular docking, 7, 2, (2019), 83-89 <https://doi.org/10.1007/s40484-019-0172-y>
- [27] Pujan N. Pandya, Sivakumar Prasanth Kumar, Kinjal Bhadresha, Chirag N. Patel, Saumya K. Patel, Rakesh M. Rawal, Archana U. Mankad, Identification of promising compounds from curry tree with cyclooxygenase inhibitory potential using a combination of machine learning, molecular docking, dynamics simulations and binding free energy calculations, *Molecular Simulation*, 46, 11, (2020), 812-822 <https://doi.org/10.1080/08927022.2020.1764552>
- [28] Dewi Astriany, Umi Baroroh, Khotibul Umam, Molecular Docking of Brazilin from Secang Wood Plant (*Caesalpinia sappan* L.) as an Anti-Breast Cancer, *al Kimiya: Jurnal Ilmu Kimia dan Terapan*, 11, 1, (2024), 68-76 <https://doi.org/10.15575/ak.v11i1.35590>
- [29] Benjamin J. Orlando, Michael G. Malkowski, Substrate-selective Inhibition of Cyclooxygenase-2 by Fenamic Acid Derivatives Is Dependent on Peroxide Tone\*, *Journal of Biological Chemistry*, 291, 29, (2016), 15069-15081 <https://doi.org/10.1074/jbc.M116.725713>
- [30] Vivek P. Chavda, Rajashri Bezbaruah, Nasima Ahmed, Shahnaz Alom, Bedanta Bhattacharjee, Lakshmi Vineela Nalla, Damanbhalang Rynjah, Laura Kate Gadanec, Vasso Apostolopoulos, Proinflammatory Cytokines in Chronic Respiratory Diseases and Their Management, *Cells*, 14, 6, (2025), 400 <https://doi.org/10.3390/cells14060400>
- [31] Max Hebditch, Jim Warwicker, Web-based display of protein surface and pH-dependent properties for assessing the developability of biotherapeutics,

- Scientific Reports*, 9, 1, (2019), 1969  
<https://doi.org/10.1038/s41598-018-36950-8>
- [32] Qian Hu, Qihui Bian, Dingchao Rong, Leiyun Wang, Jianan Song, Hsuan-Shun Huang, Jun Zeng, Jie Mei, Peng-Yuan Wang, JAK/STAT pathway: Extracellular signals, diseases, immunity, and therapeutic regimens, *Frontiers in Bioengineering and Biotechnology*, Volume 11 - 2023, (2023), <https://doi.org/10.3389/fbioe.2023.1110765>
- [33] Ruslin Ruslin, Yamin Yamin, Henny Kasmawati, Samuel Mangrura, Laode Kadidae, Armid Alroem, Muhammad Arba, The search for cyclooxygenase-2 (COX-2) inhibitors for the treatment of inflammation disease: an in-silico study, *Journal of Multidisciplinary Healthcare*, 15, (2022), 783-791  
<https://doi.org/10.2147/JMDH.S359429>
- [34] Alfonso Trezza, Anna Visibelli, Bianca Roncaglia, Roberta Barletta, Stefania Iannielli, Linta Mahboob, Ottavia Spiga, Annalisa Santucci, Unveiling Dynamic Hotspots in Protein-Ligand Binding: Accelerating Target and Drug Discovery Approaches, *International Journal of Molecular Sciences*, 26, 9, (2025), 3971  
<https://doi.org/10.3390/ijms26093971>
- [35] Masaki Tsujimura, Hiroshi Ishikita, Keisuke Saito, Determinants of hydrogen bond distances in proteins, *Physical Chemistry Chemical Physics*, 27, 18, (2025), 9794-9805  
<https://doi.org/10.1039/d5cp00511f>
- [36] Mithun Rudrapal, Wafa Ali Eltayeb, Gourav Rakshit, Amr Ahmed El-Arabey, Johra Khan, Sahar M. Aldosari, Bader Alshehri, Mohnad Abdalla, Dual synergistic inhibition of COX and LOX by potential chemicals from Indian daily spices investigated through detailed computational studies, *Scientific Reports*, 13, 1, (2023), 8656  
<https://doi.org/10.1038/s41598-023-35161-0>
- [37] Ahmed M. Said, David G. Hangauer, Binding cooperativity between a ligand carbonyl group and a hydrophobic side chain can be enhanced by additional H-bonds in a distance dependent manner: A case study with thrombin inhibitors, *European Journal of Medicinal Chemistry*, 96, (2015), 405-424  
<https://doi.org/10.1016/j.ejmech.2015.03.059>
- [38] Jason Abraham, Neha Chauhan, Supriyo Ray, Virtual Screening of Alkaloid and Terpenoid Inhibitors of SMT Expressed in *Naegleria* sp, *Molecules*, 27, 17, (2022), 5727  
<https://doi.org/10.3390/molecules27175727>
- [39] Mohamed El fadili, Mohammed Er-Rajy, Mohammed Kara, Amine Assouguem, Assia Belhassan, Amal Alotaibi, Nidal Naceiri Mrabti, Hafize Fidan, Riaz Ullah, Sezai Ercisli, Sara Zarougui, Menana Elhallaoui, QSAR, ADMET In Silico Pharmacokinetics, Molecular Docking and Molecular Dynamics Studies of Novel Bicyclo (Aryl Methyl) Benzamides as Potent GlyT1 Inhibitors for the Treatment of Schizophrenia, *Pharmaceuticals*, 15, 6, (2022), 670 <https://doi.org/10.3390/ph15060670>
- [40] Jokha Al-Qassabi, Shawn Pei Feng Tan, Patcharapan Phonboon, Aleksandra Galetin, Amin Rostami-Hodjegan, Daniel Scotcher, Facing the Facts of Altered Plasma Protein Binding: Do Current Models Correctly Predict Changes in Fraction Unbound in Special Populations?, *Journal of Pharmaceutical Sciences*, 113, 6, (2024), 1664-1673  
<https://doi.org/10.1016/j.xphs.2024.02.024>
- [41] Ekram Ahmed Chowdhury, Behnam Noorani, Faleh Alqahtani, Aditya Bhalerao, Snehal Raut, Farzane Sivandzade, Luca Cucullo, Understanding the brain uptake and permeability of small molecules through the BBB: A technical overview, *Journal of Cerebral Blood Flow & Metabolism*, 41, 8, (2021), 1797-1820  
<https://doi.org/10.1177/0271678x20985946>
- [42] A. A. Albassam, A. Ahad, A. Alsultan, H. S. Yusufoglu, A. I. Foudah, F. I. Al-Jenoobi, The inhibition of CYP1A2, CYP2C9, and CYP2D6 by pterostilbene in human liver microsomes, *Die Pharmazie - An International Journal of Pharmaceutical Sciences*, 76, 4, (2021), 155-158  
<https://doi.org/10.1691/ph.2021.1304>
- [43] Guoli Xiong, Zhenxing Wu, Jiakai Yi, Li Fu, Zhijiang Yang, Changyu Hsieh, Mingzhu Yin, Xiangxiang Zeng, Chengkun Wu, Aiping Lu, Xiang Chen, Tingjun Hou, Dongsheng Cao, ADMETlab 2.0: an integrated online platform for accurate and comprehensive predictions of ADMET properties, *Nucleic Acids Research*, 49, W1, (2021), W5-W14  
<https://doi.org/10.1093/nar/gkab255>
- [44] Syariful Anam, Yonelian Yuyun, Yusriadi Yusriadi, Asriana Sultan, David Pakaya, Saipul Maulana, Muhammad Sulaiman Zubair, Docking Study of Naphthalene Compounds from *Eleutherine Bulbosa* as Antidiabetic Agents on Multiple Receptors, *Molekul*, 20, 1, (2025), 30-38  
<https://doi.org/10.20884/1.jm.2025.20.1.10942>
- [45] Sunani Sunani, Maya Andani, Asilla Mauri Ramdini Kamaludin, Nyai Ayu Sylfia Stannia Puspitasari Helmi, Kaila Keyshia Mei, Yunitasya Guspira, Oktavia Sabetta, Diah Lia Aulifa, In Silico Study of Compounds in Bawang Dayak (*Eleutherine palmifolia* (L) Merr.) Bulbs on Alpha Estrogen Receptors, *Indonesian Journal of Cancer Chemoprevention*, 13, 2, (2022), 83-93
- [46] Antônio Rafael Quadros Gomes, Jorddy Neves Cruz, Ana Laura Gadelha Castro, Heliton Patrick Cordovil Brígido, Everton Luiz Pompeu Varela, Valdicley Vieira Vale, Liliane Almeida Carneiro, Gleison Gonçalves Ferreira, Sandro Percario, Maria Fâni Dolabela, Participation of Oxidative Stress in the Activity of Compounds Isolated from *Eleutherine plicata* Herb, *Molecules*, 28, 14, (2023), 5557  
<https://doi.org/10.3390/molecules28145557>
- [47] Kelly Cristina Oliveira de Albuquerque, Andreza do Socorro Silva da Veiga, Fernando Tobias Silveira, Marliane Batista Campos, Ana Paula Lima da Costa, Ananda Karolyne Martins Brito, Paulo Ricardo de Souza Melo, Sandro Percario, Fábio Alberto de Molfetta, Maria Fâni Dolabela, Anti-leishmanial activity of *Eleutherine plicata* Herb. and predictions of isoeleutherin and its analogues, *Frontiers in Chemistry*, 12, (2024), <https://doi.org/10.3389/fchem.2024.1341172>
- [48] Michele Pieroni, Francesco Madeddu, Jessica Di Martino, Manuel Arcieri, Valerio Parisi, Paolo Bottoni, Tiziana Castrignanò, MD-Ligand-Receptor: A High-Performance Computing Tool for Characterizing Ligand-Receptor Binding Interactions in Molecular Dynamics Trajectories, *International Journal of Molecular Sciences*, 24, 14, (2023), 11671 <https://doi.org/10.3390/ijms241411671>

- [49] Yutaka Maruyama, Ryo Igarashi, Yoshitaka Ushiku, Ayori Mitsutake, Analysis of Protein Folding Simulation with Moving Root Mean Square Deviation, *Journal of Chemical Information and Modeling*, 63, 5, (2023), 1529-1541 <https://doi.org/10.1021/acs.jcim.2c01444>
- [50] Venkatesan Saravanan, Bharath Kumar Chagaleti, Shakthi Devi Packiapalavesam, Muthukumaradoss Kathiravan, Ligand based pharmacophore modelling and integrated computational approaches in the quest for small molecule inhibitors against hCA IX, *RSC Advances*, 14, 5, (2024), 3346-3358 <https://doi.org/10.1039/d3ra08618f>
- [51] Thamir A. Alandijany, Mai M. El-Daly, Ahmed M. Tolah, Leena H. Bajrai, Aiah M. Khateb, Isra M. Alsaady, Sarah A. Altwaim, Amit Dubey, Vivek Dhar Dwivedi, Esam I. Azhar, Investigating the Mechanism of Action of Anti-Dengue Compounds as Potential Binders of Zika Virus RNA-Dependent RNA Polymerase, *Viruses*, 15, 7, (2023), 1501 <https://doi.org/10.3390/v15071501>
- [52] Ibitayo Abigail Ademuwagun, Gbolahan Oladipupo Oduselu, Solomon Oladapo Rotimi, Ezekiel Adebisi, Pharmacophore-Aided Virtual Screening and Molecular Dynamics Simulation Identifies TrkB Agonists for Treatment of CDKL5-Deficiency Disorders, *Bioinformatics and Biology Insights*, 17, (2023), <https://doi.org/10.1177/11779322231158254>
- [53] Yasmine Chemam, Samir Benayache, Abdeslem Bouzina, Eric Marchioni, Omar Sekiou, Houria Bentoumi, Minjie Zhao, Zihad Bouslama, Nour-Eddine Aouf, Fadila Benayache, Phytochemical online screening and *in silico* study of *Helianthemum confertum*: antioxidant activity, DFT, MD simulation, ADME/T analysis, and xanthine oxidase binding, *RSC Advances*, 14, 31, (2024), 22209-22228 <https://doi.org/10.1039/d4ra02540g>
- [54] Eiji Yamamoto, Takuma Akimoto, Ayori Mitsutake, Ralf Metzler, Universal Relation between Instantaneous Diffusivity and Radius of Gyration of Proteins in Aqueous Solution, *Physical Review Letters*, 126, 12, (2021), 128101 <https://doi.org/10.1103/PhysRevLett.126.128101>
- [55] Amit Kumar Srivastav, Sanjeev K. Gupta, Umesh Kumar, A molecular simulation approach towards the development of universal nanocarriers by studying the pH- and electrostatic-driven changes in the dynamic structure of albumin, *RSC Advances*, 10, 23, (2020), 13451-13459 <https://doi.org/10.1039/D0RA00803F>
- [56] Md. Mominur Rahman, Md. Junaid, S. M. Zahid Hosen, Mohammad Mostafa, Lei Liu, Kirsten Benkendorff, Mollusc-Derived Brominated Indoles for the Selective Inhibition of Cyclooxygenase: A Computational Expedition, *Molecules*, 26, 21, (2021), 6538 <https://doi.org/10.3390/molecules26216538>
- [57] Changhao Wang, D'Artagnan Greene, Li Xiao, Ruxi Qi, Ray Luo, Recent Developments and Applications of the MMPBSA Method, *Frontiers in Molecular Biosciences*, Volume 4 - 2017, (2018), <https://doi.org/10.3389/fmolb.2017.00087>
- [58] Aisyah Aisyah, Wiji Utami, Ayu Faadila, Molecular Docking and Dynamics of Bioactive Compounds Derived from *Sauropus androgynus* as Cyclooxygenase-2 Inhibitors, *Walisongo Journal of Chemistry*, 8, 2, (2025), 273-291 <https://doi.org/10.21580/wjc.v8i2.28912>
- [59] Raju Dash, Md. Chayan Ali, Nayan Dash, Md. Abul Kalam Azad, S. M. Zahid Hosen, Md. Abdul Hannan, Il Soo Moon, Structural and Dynamic Characterizations Highlight the Deleterious Role of SULT1A1 R213H Polymorphism in Substrate Binding, *International Journal of Molecular Sciences*, 20, 24, (2019), 6256 <https://doi.org/10.3390/ijms20246256>
- [60] Muharib Alruwaili, Tilal Elsaman, Magdi Awadalla Mohamed, Abozer Y. Elderderly, Jeremy Mills, Yasir Alruwaili, Siddiqa M. A. Hamza, Salma Elhadi Ibrahim Mekki, Hazim Abdullah Alotaibi, Maily J. Alrowily, Maryam Musleh Althobiti, Molecular docking, free energy calculations, ADMETox studies, DFT analysis, and dynamic simulations highlighting a chromene glycoside as a potential inhibitor of PknG in *Mycobacterium tuberculosis*, *Frontiers in Chemistry*, Volume 13 - 2025, (2025), <https://doi.org/10.3389/fchem.2025.1531152>
- [61] Riyan Alifbi Putera Irsal, Gusnia Meilin Gholam, Maheswari Alfira Dwicesaria, Fernanda Chairunisa, Computational investigation of *Y. aloifolia* variegata as anti-Human Immunodeficiency Virus (HIV) targeting HIV-1 protease: A multiscale *in-silico* exploration, *Pharmacological Research - Modern Chinese Medicine*, 11, (2024), 100451 <https://doi.org/10.1016/j.prmcm.2024.100451>